

## Measurement results of the power of radiation losses and effective ion charge in experiments on the Globus-M2 tokamak

E. Tukhmeneva, N. Bakharev, V. I. Varfolomeev, V. K. Gusev,

N. S. Zhiltsov, E. O. Kiselev, G. S. Kurskiev, V. B. Minaev, Yu. V. Petrov,

N. V. Sakharov, A. Yu. Telnova, S. Yu. Tolstyakov, P. B. Shchegolev

*Ioffe Institute, St. Petersburg, Russia*

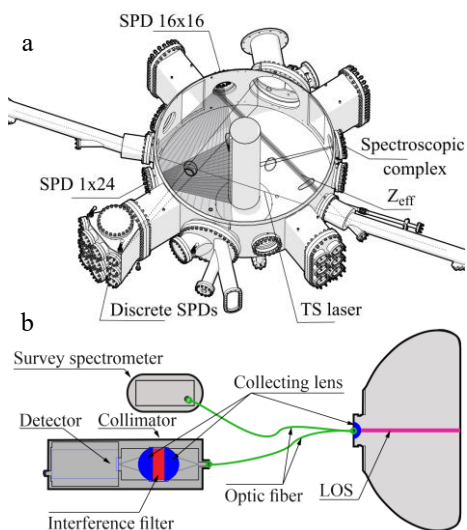


Fig.1. The diagnostic complex on Globus-M2; b) the schematic of the spectroscopic diagnostics.

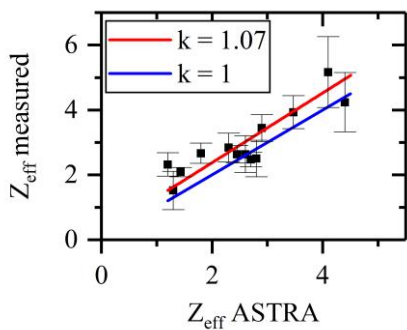


Fig.2. Correlation between  $Z_{\text{eff}}$  from bremsstrahlung and  $Z_{\text{eff}}$  obtained by ASTRA simulation.

The values of  $Z_{\text{eff}}$  are determined from the analysis of the intensity of bremsstrahlung radiation  $P_{\text{br}}$  in three spectral intervals 1019-1040 nm, 1040-1049 nm and 948-952 nm along one line-of-sight in the equatorial section of the tokamak vessel using a filter monochromator based on an APD detector (a Hamamatsu S11519-30) (figure 1a) [2]. The simulation results obtained by ASTRA [6] modelling show good agreement between calculated and experimental  $Z_{\text{eff}}$  values (fig.2). The spectroscopic diagnostics [4] of impurities consists of survey spectrometer

1) *The diagnostic complex.* The Globus-M2 tokamak (the Unique Scientific Facility ‘Spherical tokamak Globus-M’, which is incorporated in the Federal Joint Research Center “Material science and characterization in advanced technology”) is a spherical tokamak with the toroidal magnetic field  $B_T$  up to 1 T, the plasma current  $I_p$  up to 0.5 MA, the electron temperature  $T_e$  up to 1.5 keV and the range of average electron densities  $\langle n_e \rangle$  of  $2 \cdot 10^{19} \text{ m}^{-3}$  [1]. To search for a way to improve energy confinement, it is necessary to study the processes affecting it - energy transport, occurrence of instabilities, contamination by impurities. The transport of impurities in plasma is studied using a diagnostic complex (figure 1a) consisting of effective ion charge  $Z_{\text{eff}}$  diagnostics [2], diagnostics of radiation losses  $P_{\text{rad}}$  [3] and spectroscopic diagnostics [4] (Figure 1b). Multi-chord measurements by arrays of SPD photodiodes [5] are used to reconstruct the two-dimensional distribution of  $P_{\text{rad}}$  in poloidal section [3].

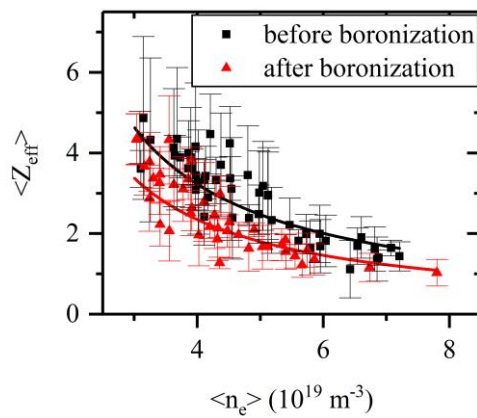


Fig. 3.  $\langle Z_{\text{eff}} \rangle$  dependence on  $\langle n_e \rangle$  for discharges with the same parameters ( $B_T = 0.8 \text{ T}$  and  $I_p = 400 \text{ kA}$ , with NBI and limiter configuration) before and after boronization.

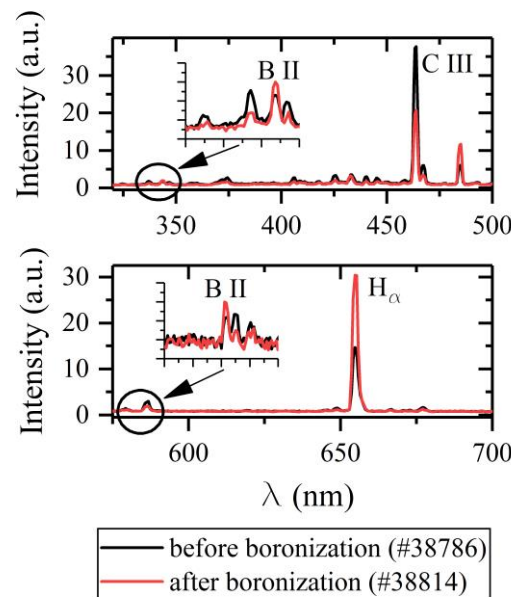


Fig. 4. Survey spectra before boronization (#38786) and after boronization (#38814) for  $t = 0.162 \text{ s}$ .

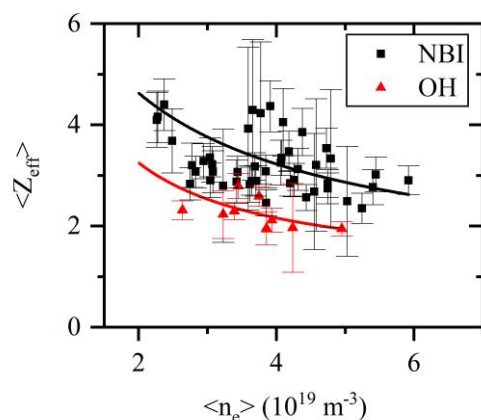


Fig. 5.  $\langle Z_{\text{eff}} \rangle$  dependence on  $\langle n_e \rangle$  for OH and NBI heating in the same discharges with  $B_T = 0.8 \text{ T}$  and  $I_p = 0.4 \text{ kA}$  after boronization.

6). Also, the effect of neutral beam injection can be seen in the diagnostics of radiation losses.

Avaspec-2048 to detect radiation from plasma in the spectral range of 200-1100 nm every 20 ms during the discharge and monitoring system registered individual spectral lines of impurity elements C III, O II, Fe I, N II, the schematic of the spectroscopic diagnostics is demonstrated on picture 1b. Individual lines intensities are measured by filter monochromators based on PMT Hamamatsu H10721-20 and semiconductor detectors FPU2-153.

2) *Experimental results.* The borocarbon film deposition on the surface (boronization) in a glow discharge in a mixture of helium and carborane vapour [7] is periodically used for vacuum vessel conditioning. The effect of boronization on the impurity content in the plasma was estimated using the data of  $Z_{\text{eff}}$  diagnostics and spectroscopic diagnostics. A decrease in the impurities content after boronization is registered by a survey spectrometer (less by 40% for CIII), C III line monochromator (less by 25%),  $Z_{\text{eff}}$  diagnostics (less by 30%) – see figures 3 and 4.

A neutral beam injection (NBI) is used on Globus-M2 as one of the additional heating method. The  $Z_{\text{eff}}$  was measured in the regimes with ohmic and NBI heating. As we can see in figure 5,  $Z_{\text{eff}}$  is 30-50% higher in discharges with additional heating by NBI than in ohmic discharges. An increasing the intensity of emission lines of impurities by about 45% is registered by the survey spectrometer and monitoring lines monochromators (CIII in figure

Figure 6 and 7 demonstrates that the radiation power to input power ratio  $P_{\text{rad}} / P_{\text{in}}$  ( $P_{\text{in}}$  is composed of two components: ohmic heating and power absorbed by plasma from the NBI) rises with beginning of NBI. The total power of radiation losses increases linearly with the increase in the electron density [8, 9]. But an increase in the intensity of the impurity influx is associated not only with an increase in density (plasma interacts more actively with the wall at high densities), but also with the interaction of the neutral beam with the chamber wall.

3) *The diagnostic complex upgrade.* The diagnostic complex is being modernized and expanded to further study the transport processes at the Globus-M2 facility. Firstly, the installation of new monochromators for recording the intensities of He II, B II, Cu II lines will

be carried out in the near future. In addition, the SPD system will operate in a new geometry, in which all registration chords lie in one poloidal cross-section (Figure 8a).

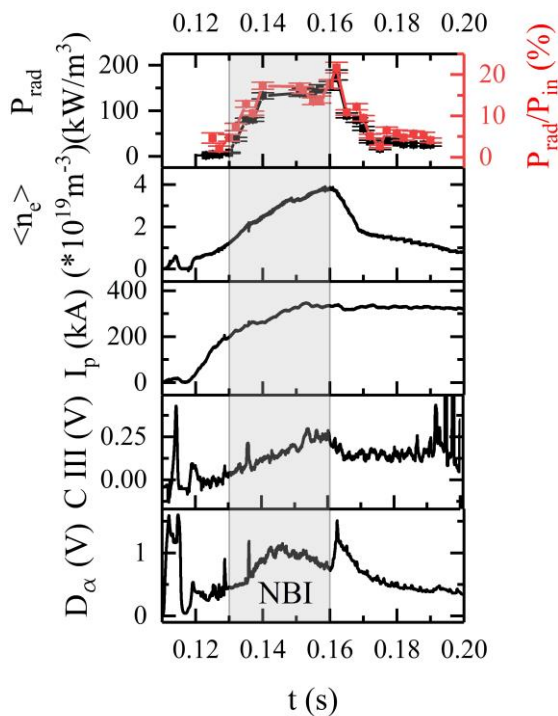


Fig. 6. Evolution of absolute  $P_{\text{rad}}$  and  $P_{\text{rad}}/P_{\text{in}}$  with parameters of discharge #38404.

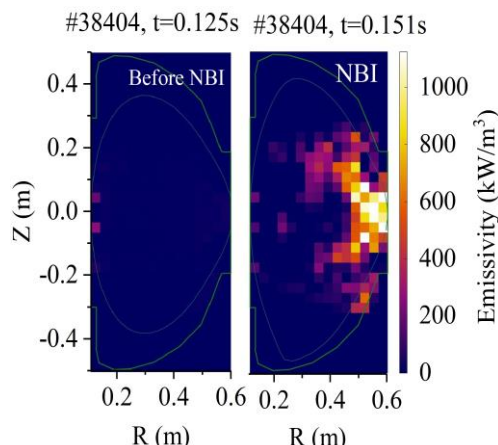


Fig. 7. 2D distribution of radiation losses before and during NBI.

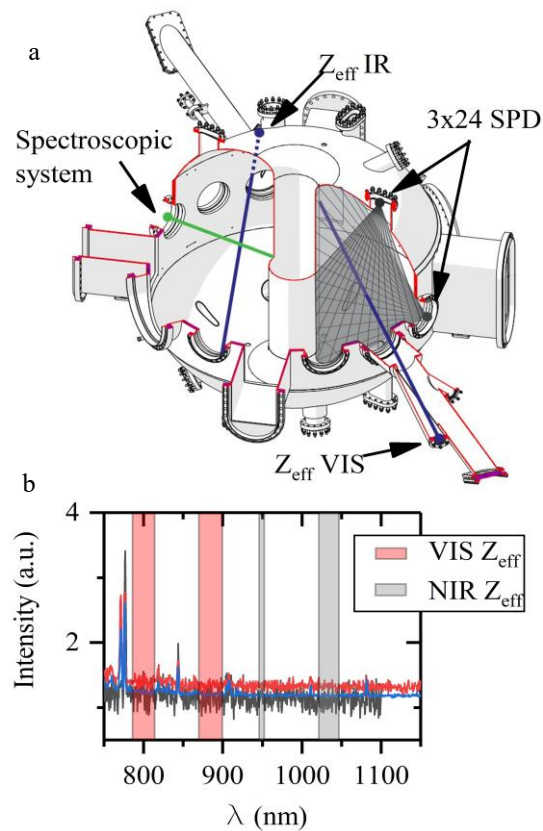


Fig. 8. a) New geometry of diagnostic system; b) Spectral intervals for measurements of  $P_{\text{br}}$  in VIS and IR spectral range.

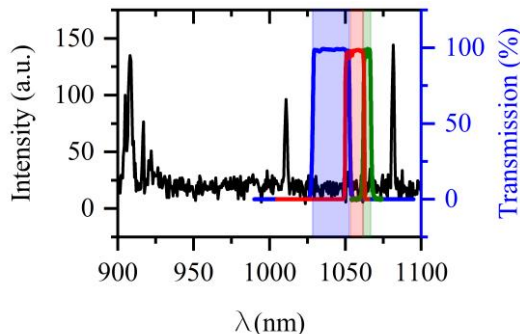


Fig. 9. Spectral channels of TS polychromator suitable for  $P_{br}$  measurements.

The SPD system will include one pair of SPD linear arrays without filters for  $P_{rad}$  measurements in a wide spectral range and two pairs of SPD linear arrays with 50  $\mu\text{m}$  and 100  $\mu\text{m}$  beryllium filters for SXR and  $T_e$  measurements. The new approach will allow to study of MHD activity, snake and sawtooth instabilities, IRE (since lines-of-sight lie in one

section, it is possible to research toroidally asymmetric phenomena), radiation from divertor and detachment.  $Z_{eff}$  diagnostics will be completed with a second monochromator for measurements of  $P_{br}$  along the new line-of-sight (figure 8a) in the visible spectral range (Figure 8b). Simultaneous  $Z_{eff}$  measurements using both VIS and NIR monochromators will be used to provide cross-validation of results. Also three channels (figure 9) of the TS [10] diagnostic polychromator will be additionally used to detect  $P_{br}$ . Multi-chord measurements along the 10 chords of TS system will be used to obtain the  $Z_{eff}$  ( $R$ ) profile. The combined use of diagnostics of radiation losses, effective plasma charge, and a new spectroscopic system made it possible to apply a combine approach to studying the behaviour of an impurity.

Experiments on magnetic confinement on Globus-M2 presented in section 1 and experiments on NBI heating presented in section 2 were made within the frameworks of Programs of scientific research of state academies of sciences № 0040-2019-0023 and № 0034-2021-0001 respectively. The research of impurities and modernization of diagnostic complex presented in section 3 was carried out with the financial support of the Russian Foundation for Basic Research, project No. 20-32-90183.

#### References

- [1] Minaev V. B. et al 2018 J. Phys.: Conf. Ser. 1094 012001.
- [2] Sladkomedova et A. D. al, Rev. Sci. Instrum. 89, 083509 (2018).
- [3] Tukhmeneva E. A. et al 2019 Plasma Sci. Technol. 21 105104.
- [4] Tukhmeneva E.A // INTERNATIONAL CONFERENCE ON PLASMA PHYSICS AND CONTROLLED FUSION 15 - 19 March, 2021.
- [5] Artyomov A. P. et al, Instrum. Exp. Tech. 58, 102 (2015).
- [6] Pereverzev G V Yushmanov P N 2002 IPP 5/98
- [7] Gusev V. K. et al, Nucl. Fusion 41, 919 (2001).
- [8] Tukhmeneva, E.A. et al. Tech. Phys. Lett. 47, 56–60 (2021).
- [9] Marrelli L. et al. Nucl. Fusion 38 649 (1998).
- [10] Zhiltsov N.S. // INTERNATIONAL CONFERENCE ON PLASMA PHYSICS AND CONTROLLED FUSION 15 - 19 March, 2021.